Proceedings of the Institute of Acoustics

ADAPTIVE FEEDFORWARD CONTROL OF FLEXURAL WAVES PROPAGATING IN A BEAM

S.J. Elliott, I.M. Stothers and L. Billet

Institute of Sound and Vibration Research, University of Southampton, Southampton S09 5NH, England.

INTRODUCTION

The principle of actively controlling flexural (bending) waves propagating in a beam using feedforward control can be understood by analogy with the control of plane sound waves propagating in a duct [1]. The incident flexural wave is detected with an array of detection sensors whose signals are fed through a matrix of electronic control filters and fed to an array of secondary sources exciting the beam further downstream. The problem of controlling flexural waves is more complicated than the analogous acoustic problem, however, because of two features of such wave motion: (a) the generation of such waves involves an evanescent, near field, component which is strong at low frequencies, and (b) the propagation is dispersive. Various arrangements of detection sensors and secondary sources have been suggested for such a control system. The simplest involves a single measurement of beam motion fed forward to a single control force [2]. Such an arrangement is capable of reflecting the propagating component of wave motion, but a near field component is still present on both sides of the secondary source, and the flexural wave amplitude may be increased on the upstream side of the secondary source because of standing wave effects. A control system with two control forces can be arranged to *either* control the propagating and near field components downstream of the secondary source array [3,4] in which case the flexural wave is still reflected back upstream, *or* the two control forces can be arranged to absorb the propagating wave component [2,5] in which case residual near field components will still be present on both the downstream and upstream sides of the secondary source array. Four properly driven force inputs would be required to both absorb the incoming flexural wave and not generate any near fields beyond the source array [2].

Previous methods of designing the response of the electronic controller required in such active control systems have involved the frequency domain manipulation of individually measured or calculated transfer functions. The object of this work was to investigate the use of adaptive digital filters in implementing the required controller. To keep the experimental arrangement as simple as possible a single accelerometer was used as the detection sensor and a single electrodynamic actuator used as the secondary source. The active control system investigated is illustrated in Figure 1(a), in which $x(t)$ is the signal from the detection sensor, $y(t)$ is the signal driving the secondary source from the electronic controller, which has a frequency response $T(j\omega)$, and $e(t)$ is the signal from the error sensor. The equivalent block diagram for the physical arrangement of Figure 1(a) is shown in Figure 1(b), in which $X(\omega)$, $Y(\omega)$ and $E(\omega)$ are the Fourier transforms of the signals $x(t)$, $y(t)$ and $e(t)$. The contribution from the primary source to the detection sensor output is $I(\omega)$ and that to the error sensor is $D(\omega)$. The purely electrical frequency responses, which contain the various electromechanical paths are defined as:

$$C(j\omega) = \left.\frac{E(\omega)}{Y(\omega)}\right|_{I(\omega)=0}, \quad F(j\omega) = \left.\frac{X(\omega)}{Y(\omega)}\right|_{I(\omega)=0} \quad \text{and} \quad P(j\omega) = \left.\frac{E(\omega)}{X(\omega)}\right|_{T(j\omega)=0},$$

which are referred to as the error path, feedback path and primary path, respectively. It is assumed that no measurement noise is present at either the detection or error sensor.

The physical consequences of using a single detection sensor, secondary source and error sensor are investigated in the next section and some experimental results obtained by implementing such a control system are then reported.

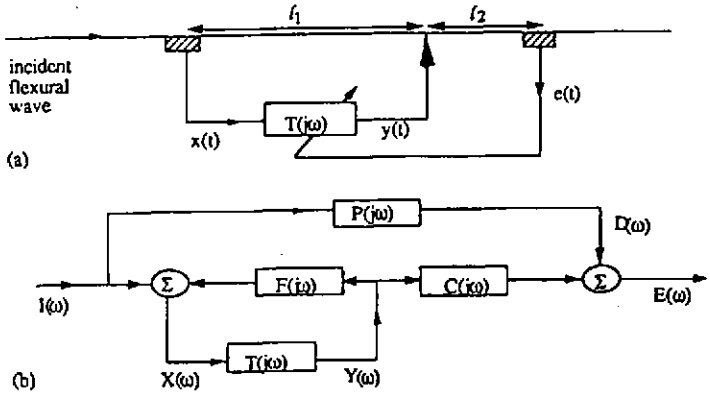

Figure 1. The physical arrangement of the active control system (a) and its equivalent electrical block diagram (b).

THE THEORETICAL FORM OF THE CONTROLLER

The total error signal can be deduced from Figure 1(b) as

$$E(\omega) = \left[P(j\omega) + \frac{C(j\omega)T(j\omega)}{1 - T(j\omega)F(j\omega)}\right] I(\omega)$$

In the case of no measurement noise, this error signal can be driven to zero if the controller response is

$$T_0(j\omega) = \frac{-P(j\omega)}{C(j\omega) - P(j\omega)F(j\omega)}$$

ADAPTIVE CONTROL OF FLEXURAL WAVES

The purpose of this section is to investigate the physical form of the individual frequency responses $P(j\omega)$, $C(j\omega)$ and $F(j\omega)$ in the case of bending waves propagating in a beam and so calculate the theoretical form for the optimal controller in this case.

The Bernoulli-Euler wave equation for harmonic flexural waves propagating in a uniform one-dimensional structure with spatial coordinate x can be expressed as [6]

$$EI\frac{\partial^4 w(x)}{\partial x^4} - \omega^2 m w(x) = f(x)$$

where EI is the bending stiffness of the beam and m its mass per unit length, $w(x)$ the transverse displacement at a position x and frequency ω and $f(x)$ the force per unit length applied at position x and frequency ω. For a harmonic point force input $fe^{j\omega t}$ applied to an infinite beam at the origin of the coordinate system, the resulting displacement at a position $x > 0$ can be written [6]

$$w(x) = \frac{-jf}{4EIk^3}\left[e^{-jkx} - je^{-kx}\right]$$

where k is the wavenumber which is equal to

$$k = \left(\frac{m}{EI}\right)^{1/4}\omega^{1/2} \Rightarrow \left(\frac{12\rho}{Eh^2}\right)^{1/4}\omega^{1/2}$$

where the second expression refers to a thin beam of thickness h, Young's modulus E and density ρ. The secondary force generated by a coil and magnet can be considered to be acting at a point at the origin of the coordinate system with a magnitude given by $BLY(\omega)/Z_e(j\omega)$ where B is the flux density of the magnet, L the length of wire in the coil, $Y(\omega)$ the electrical voltage applied to the coil, at frequency ω, and $Z_e(j\omega)$ its electrical impedance at this frequency. The detection and error sensors are assumed to measure the acceleration of the beam, which when excited by the coil and magnet will be

$$\ddot{w}(x) = H_s Y(\omega)\left[e^{-jk|x|} - je^{-k|x|}\right]$$

where $H_s = \dfrac{j\omega^2 BL}{4EIk^3 Z_e(j\omega)}$. The electrical signals from the detection and error sensors can be expressed as

$$X(\omega) = H_x\ddot{w}(-l_1) \text{ and } E(\omega) = H_e\ddot{w}(l_2)$$

where H_x and H_e are calibration factors of the transducers which, to a first approximation, are frequency independent. The frequency responses of the error and feedback path on an infinite beam can now be expressed as

$$C(j\omega) = \frac{E(\omega)}{Y(\omega)} = H_c H_s[e^{-jk\ell_2} - je^{-k\ell_2}]$$

$$F(j\omega) = \frac{X(\omega)}{Y(\omega)} = H_x H_s[e^{-jk\ell_1} - je^{-k\ell_1}]$$

If the detection sensor and error sensor are far from any discontinuities in the beam and are subject to a harmonic bending wave excitation from the downstream end of the beam, whose nearfield component has died away, then

$$P(j\omega) = \frac{H_e}{H_x} e^{-jk(\ell_1+\ell_2)}$$

Substituting these expressions into the expression for the optimal controller, we obtain

$$T_0(j\omega) = \frac{1}{H_x H_s} \frac{-e^{-jk(\ell_1+\ell_2)}}{(e^{-jk\ell_2} - je^{-k\ell_2}) - e^{-jk(\ell_1+\ell_2)}(e^{-jk\ell_1} - je^{-jk\ell_1})}$$

The control objective of driving the error signal to zero will drive the *sum* of the propagating and evanescent components to zero. The acceleration at the error sensor, assuming it is remote from any discontinuity, could be written as

$$\ddot{w}(\ell_2) = Ae^{-jk\ell_2} + B(e^{-jk\ell_2} - je^{-k\ell_2})$$

where A is the incident bending wave amplitude as it passes the secondary source and B is the contribution from the secondary source. If $\ddot{w}(\ell_2)$ is driven to zero then

$$B = -Ae^{-jk\ell_2}/(e^{-jk\ell_2} - je^{-k\ell_2})$$

The residual *propagating* wave amplitude will be equal to $A + B$, and so the ratio of this to the original incident wave amplitude is

$$\frac{A+B}{A} = \frac{-je^{-k\ell_2}}{(e^{-jk\ell_2} - je^{-k\ell_2})}$$

This equation will set the fundamental limits on the attenuation of the propagating flexural waves using an active control system with a single error sensor. For the beam used in the experiments below (which was 6 mm thick steel with $\ell_2 = 0.7$ m) this maximum achievable attenuation of a propagating flexural wave has been calculated at various frequencies and is plotted on Figure 2. It can be seen that, provided attenuations of no more than 20 dB are anticipated (a reasonable ambition in practice), the near field of the secondary source only degrades the performance of the active control system below about 20 Hz.

ADAPTIVE CONTROL OF FLEXURAL WAVES

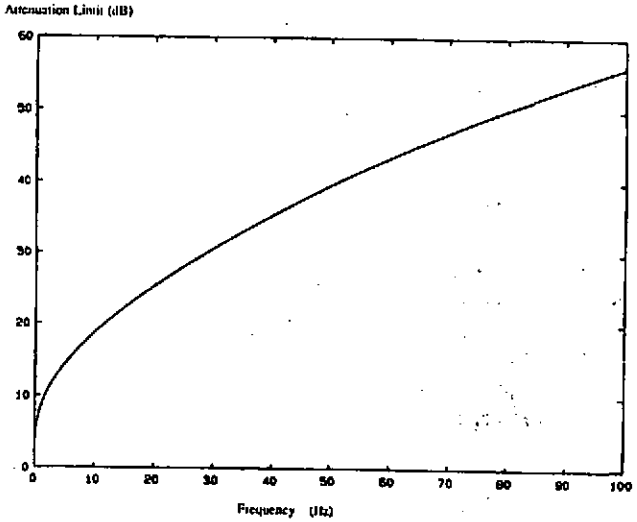

Figure 2. Maximum attenuation of a propagating flexural wave in the beam below, using a control system with a single error sensor, due to the nearfield of the secondary source.

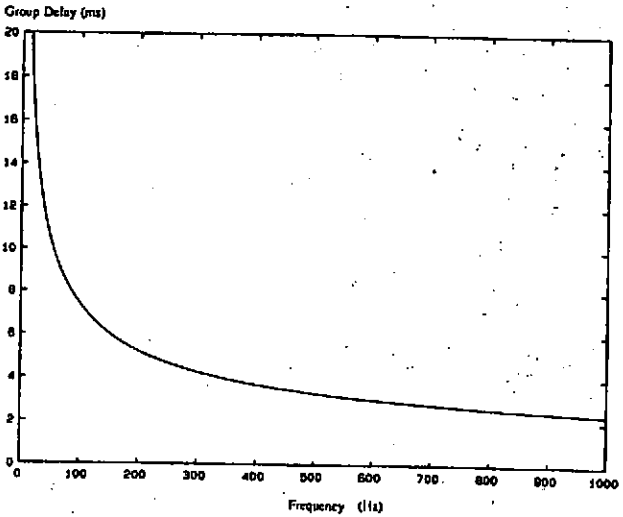

Figure 3. The group delay of a flexural wave propagating from the detection sensor to the secondary source for the beam below.

For frequencies above about 20 Hz, then, the evanescent component of the flexural wave from the secondary source at the error sensor can, to a reasonable approximation, be ignored. The same is also true of the near field contribution from the secondary source at the detection sensor, if $\ell_1 = \ell_2$. The frequency response of the optimal controller then reduces to

$$T_0(j\omega) = \frac{1}{H_x H_s} \frac{e^{-jk\ell_1}}{1 - e^{-jk2\ell_1}}$$

which is of exactly the same form as that in the acoustic case [7]. The difference here, however, is that the wavenumber is frequency dependent, so the Fourier transform of terms of the form $e^{-jk\ell}$ are not just simple time delays, and the controller does not have a simple time-domain interpretation. The effect of this dispersion is that the velocity of the bending waves increases with frequency, and so the group delay, τ_g, of the bending wave between any two points a distance ℓ apart on a thin beam decreases with frequency according to the expression

$$\tau_g = \ell \frac{\partial k}{\partial \omega} = \frac{\ell}{2}\left(\frac{12\rho}{Eh^2}\right)^{1/4} \omega^{-1/2}$$

The electrical controller has to model a rather complicated frequency response and the most accurate and flexible way of implementing such a controller is using digital filters. Such digital controllers have a certain inherent delay associated with them partly due to the phase lag in the analogue antialias and reconstruction filters, and partly due to the processing time of the device performing the digital filtering operation. When this electrical delay is greater than the time taken for the flexural wave to propagate from the detection sensor to secondary source it will not be possible to achieve cancellation of an incident field of random waveform. The appropriate group delay for the beam used below, 6 mm steel with $\ell_1 = 1$ m, is plotted as a function of frequency in Figure 3. For an electrical processing delay of 4 ms (as measured in the control system used in the next section), this graph suggests that attenuation of random incident waves will not be possible above about 400 Hz. It has also been pointed out [8] that a finite impulse response filter will not be able to control the very low frequency components due to their very large delays. The maximum delay in the FIR filter used below was about 100 ms, corresponding to a lower cut-off frequency of about 0.5 Hz. This is clearly an even lower frequency limit than that set by the effect of the near field on the error sensor.

EXPERIMENTS

The experiments were performed on a 6 mm × 50 mm steel beam of total length 6.2 m. The final 1 m of beam at either end was inserted into a sand box to give an available length of 4.2 m. The effect of the sand boxes was to make the beam appear almost anechoic above about 200 Hz, although individual resonances could be seen in the beam's response below this frequency. The primary excitation was generated by a coil and magnet

arrangement 0.26 m from one sand box, the detection sensor (B & K type 4375 accelerometer) placed 0.85 m beyond this, with the coil and magnet secondary source positioned a distance (ℓ_1) of 1.0 m from the detection sensor. The error sensor (B & K type 4374 accelerometer) was positioned 0.7 m from the secondary source (ℓ_2). The primary source was driven by a white noise generator which produced a power spectrum at the error sensor as shown in Figure 4. The output from the detection sensor was passed through an anti-aliasing filter (Kemo type VBF/23 with a cut-off frequency of 800 Hz) and fed to a 12 bit analogue-to-digital converter which was part of a real time signal processing system (Loughborough Sound Images PCS25 and PC4i2o, resident in a PC) operating at a sample rate of 2kHz. The signal processor implemented a "feedback cancellation" architecture of controller [9] in which the feedback path is modelled with one digital filter (with 200 coefficients) prior to control, and during the control phase this model of the feedback path is arranged to be in parallel and out of phase with the physical feedback path. Such an arrangement is known as an Echo Canceller in the telecommunications literature [10]. The output from the controller is passed through a 12 bit digital-to-analogue converter and reconstruction filter and fed via a voltage amplifier to the coil and magnet acting as the secondary source. The signal from the error sensor is also fed to the controller and used to update the feedforward path, an FIR filter with 200 coefficients, during control by implementing the "filtered x LMS" adaptive algorithm [11].

The power spectrum at the error sensor after control is also shown in Figure 4 and it can be seen that reductions in the level of this spectrum have been achieved from about 100 Hz to 600 Hz with 15 to 20 dB of attenuation from about 120 Hz to 400 Hz. The high frequency limit of performance is very much as predicted in the previous section, as being due to the overall delay in the digital controller exceeding the group delay in the beam above about 400 Hz. What was not predicted, however, was the lack of attenuation below 100 Hz. Further investigation revealed that the performance in this region was fundamentally limited by the lack of coherence between the detection and error sensors ($\gamma^2_{xe}(\omega)$). The minimum level of the power spectral density at the error microphone ($S_{ee}(\omega)$) achievable with a linear time invariant controller can be shown to be [12]:

$$S_{ee}(\omega)_{min} = [1 - \gamma^2_{xe}(\omega)]S_{ee}(\omega)_{primary}.$$

This function is conveniently computed as "non-coherent power" on some two channel analysers, and was measured in the experiment above and plotted, together with the original power spectral density at the error microphone ($S_{ee}(\omega)_{primary}$), in Figure 5. This theoretically minimum level is seen to be very similar to the minimum levels achieved in practice below about 200 Hz, suggesting that below this frequency the controller is fundamentally limited by the noise and nonlinearities in the system. Below 100 Hz very little change is observed in the error spectrum as a result of active control and the controller response must be very small in this frequency range. Any limitation imposed below 20 Hz by the near field from the secondary source impinging on the error microphone is therefore not observed in this experiment.

One disadvantage of the feedback cancellation architecture of controller is that both the feedforward and feedback filters in the controller are strongly affected by reflections from either end of the beam, which tend to make their impulse responses longer than they need

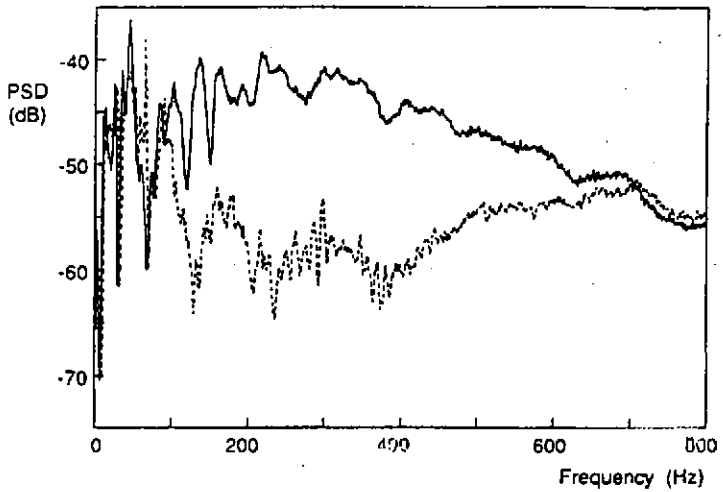

Figure 4. The measured power spectral density of the signal from the error sensor before (solid) and after (dashed) convergence of the active control system.

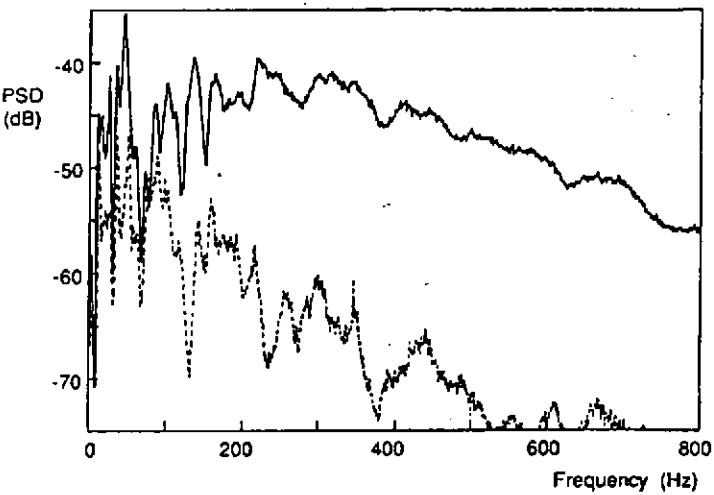

Figure 5. The measured power spectral density of the signal from the error sensor (solid) and the "non-coherent power" associated with this signal compared with that from the detection sensor (dashed).

otherwise be. If the feedback path were perfectly cancelled the frequency response of the feedforward path of the controller in an *infinite* beam would be given by

$$T(j\omega) = \frac{-P(j\omega)}{C(j\omega)} \Rightarrow -\frac{e^{-jkf_1}}{H_x H_s}$$

where nearfield terms from the secondary source have been ignored. The inverse Fourier transform of this frequency response, calculated using the expression for H_s derived in the section above, is compared with the measured impulse response of the converged feedforward path of the controller in Figure 6. An additional delay of 4 ms has been added to the response of the measured feedforward path to account for the delays in the analogue filters and digital processor, as discussed above. The general form of the two responses are seen to be in good agreement, with extra detail in the measured response being due to reflections on the beam used for the experiments.

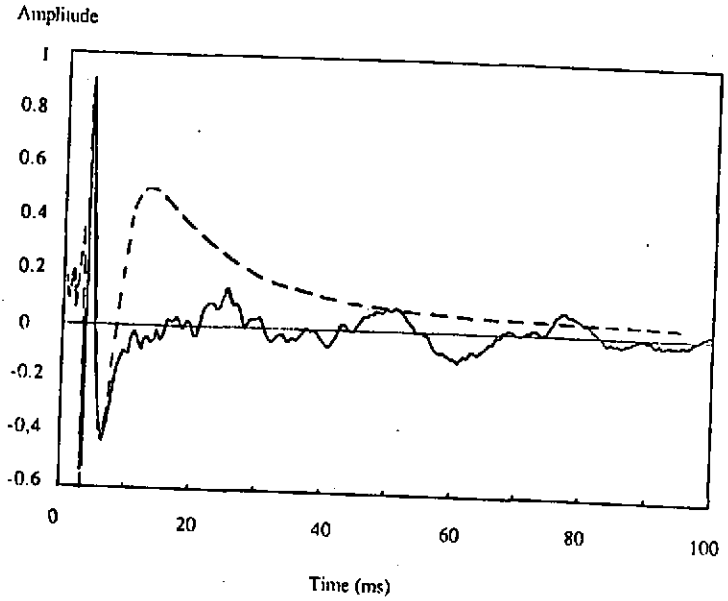

Figure 6. *The measured impulse response of the feedforward path on the beam, with an additional 4 ms of processing delay (solid line) and calculated impulse response for a control system operating on an infinite beam (dashed line).*

CONCLUSIONS

A single channel active control system for reflecting flexural waves propagating in a beam has been studied. The use of a single error sensor is seen to impose a low frequency limit on the attenuation of the propagating component of the flexural wave because of the near field of the secondary source. The increasing wave velocity with frequency is seen to impose a high frequency limit on the action of the active control system because of the inherent delay in a digital controller. The frequency range of operation for the beam used in the experiments (6 mm thick steel) was calculated as being from about 20 Hz to 400 Hz. For a thinner beam the lower frequency limit would fall, the upper frequency limit rise and the usable bandwidth increase.

The electronic controller required in this application has a rather complicated impulse response, but significant reductions in the error signal were obtained experimentally by using an adaptive filter to automatically adjust its response to minimise the mean square value of this signal. Although attenuations of 15-20 dB were measured up to 400 Hz, with gradually diminishing attenuations up to 700 Hz, a lower limiting frequency of operation of about 100 Hz was observed. This lower limiting frequency was found to be due to a lack of coherence between the signals from the detection and error sensors. The measured response of the controller was similar to the theoretically calculated response.

REFERENCES

1. M.A. SWINBANKS 1973 *Journal of Sound and Vibration* **27**, 411-436. The active control of sound propagating in long ducts.
2. J. SCHEUREN 1985 *Proc. Inter-Noise 85* , 591-595. Active control of bending waves in beams.
3. R.B. MACE 1987 *Journal of Sound and Vibration* **114**, 253-270. Active control of flexural vibrations.
4. R.J McKINNELL 1988 *Proc. Institute of Acoustics* **10**, 581-588. Active vibration isolation by cancelling bending waves.
5. A.R.D. CURTIS 1988 *Ph.D. Thesis, University of Southampton.* The theory and application of quadratic minimisation in the active reduction of sound and vibration.
6. M.C. JUNGER and D. FEIT 1986 *Sound, Structures and their Interaction,* 2nd edition. MIT Press.
7. A. ROURE 1985 *Journal of Sound and Vibration* **101**, 429-441. Self adaptive broad band sound control system.
8. J. SCHEUREN 1989 *Proc. ICASSP* paper A2.3. Iterative design of bandlimited FIR-filters with gain constraints for active control of wave propagation.
9. L.A. POOLE, G.E. WARNAKA and R.C. CUTTER 1984 *Proc. ICASSP* paper 21.7. The implementation of digital filters using a modified Wiener-Hoff algorithm for the adaptive cancellation of acoustic noise.
10. M.M. SONDHI and D.A. BERKLEY 1980 *Proc. IEEE* **68**, 948-963. Silencing echoes on the telephone network.
11. B. WIDROW and S.D. STEARNS 1985 *Adaptive Signal Processing.* Prentice Hall.
12. P.A. NELSON, T.J. SUTTON and S.J. ELLIOTT 1990 *Proc. IOA Spring Conference,* Southampton. Performance limits for the active control of random sound from multiple primary sources.